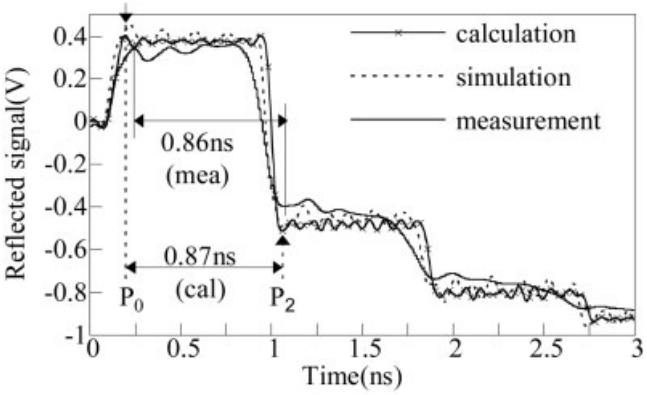


**Figure 5** Calculated, simulated, and measured reflection signals for $\varepsilon_r = 3.0$ and excitation of a rectangular pulse

### 3. CALCULATION, SIMULATION, AND EXPERIMENT

For verification of the analysis procedure and results, several probes are simulated in time domain using the time domain EM simulator, the CST Microwave Studio [5]. A prototype, $a = 0.63$ mm, $b = 15$ mm, and $L = 75$ mm is fabricated. In Figure 3, a photograph of the fabricated probe is displayed. It can be shown that the metal top has a hole to fit the inner metal core.

For measurement, a TDR meter, LeCroy SDA 100G using a rectangular step pulse is used. As a test material, dry sand of diameter less than 0.5 mm is used. For preparing test sand of different dielectric constant, moisture content of the sand is adjusted for the desired dielectric constant, and for a relation between moisture content and bulk dielectric constant, the following result in [3] is used.

$$\theta_v = -5.3 \times 10^{-2} + 2.92 \times 10^{-2}\varepsilon_r - 5.5 \times 10^{-4}(\varepsilon_r)^2 + 4.3 \times 10^{-6} \cdot (\varepsilon_r)^3 \quad (6)$$

where $\theta_v$ is moisture content.

In Figure 4, the calculated reflection waveforms for exciting a Gaussian pulse of 50 ps rising time are displayed for three different dielectric constants ($\varepsilon_r = 1, 3, 5$). For the calculation, propagation modes of TEM and $TM_{01}$ are considered. As is shown, the first reflections of three materials which occur at the discontinuity ($z = 0$) between SMA connector and probe are observed at $P_0 = 0.2$ ns (nanosecond, $10^{-9}$ s). The points of the second reflections are dependent on the dielectric constants. For the case of $\varepsilon_r = 3.0$, the point of the second reflection $P_2$ is 1.07 ns. Thus, using (5) yields bulk dielectric constant of $\varepsilon_r = 3.0$. It should be noted that the other reflected signals have negative polarity because the points of $P_1$, $P_2$, and $P_3$ occur at the metal top. The point of $P_{12}$ occurs at $z = 0$ by reflection of the signal which is reflected at the metal top for $\varepsilon_r = 1.0$. It can be also seen that ripples in the reflection waveforms due to the higher mode of $TM_{01}$ are observed for each dielectric constant.

Figure 5 shows calculation, simulation, and measurement of the probe for $\varepsilon_r = 3.0$ and excitation of a step pulse. The input step pulse has 50 ps rising time and amplitude "1." Using (5), measured dielectric constant of 3.02 and calculated dielectric constant of 2.96 are obtained, respectively. As is shown, the calculated result agrees well with the simulation and measurement in terms of dielectric constant while the amplitude of reflected signal is slightly different from the measurement. Ripples in the reflected step pulses are also observed due to propagation of higher modes and the ripples make the reflection point of each waveform less clear than that in Figure 4. Thus, it is necessary to reduce higher modes propagating in the probe for better time resolution of the probe in TDR applications using excitation of a step pulse. In addition, it should be noted that calculation, simulation, and measurement are converging on amplitude "−1." The reason is that the input signal is reflected at the metal top and the metal plate at $z = 0$ as explained in Figure 4.

### 4. CONCLUSION

A short-ended cylinder probe is analyzed in time domain for TDR applications to bulk dielectric constant measurement of porous media. From calculation and measurement, time domain analysis results agree well with measurement. It is also found that the probe may have better time resolution by stopping propagation of higher modes in the probe and then reducing ripples by the higher modes. It is expected that due to much simpler configuration of the proposed probe, it can be easily made and widely used for practical TDR applications. In addition, the proposed probe and analysis method can be applied to design a short-ended probe for different TDR applications such as a liquid level sensor.

### REFERENCES

1. S.B. Jones, J.M. Wraith, and D. Or, Time domain reflectometry measurement principles and applications, Hydrological Process 16 (2002), 141–153.
2. B.P. Kwok, S.O. Nelson, and E. Bahar, Time-domain measurements for determination of dielectric properties of agricultural materials, IEEE Trans Instrum Meas IM-28 (1979), 109–112.
3. G.C. Topp, J.L. Davis, and A.P. Annan, Electromagnetic determinations of soil water content: Measurements in coaxial transmission lines, Water Resources Res 16 (1980), 574–582.
4. J.R. Andrews, Time domain reflectometry (TDR) and time domain transmission (TDT) measurement fundamentals, Application note AN-15, Picosecond Pulse Labs, Boulder CO, 2004.
5. CST Microwave Studio (CST MWS), version 2008, CST GmbH, Germany.
6. R.F. Harrington, Time-harmonic electromagnetic fields, McGraw-Hill, NY, 1961.
7. N. Marcuvitz, Waveguide handbook. McGraw-Hill, NY, 1951.



## PRINTED DOUBLE-T MONOPOLE ANTENNAS FOR TRIBAND APPLICATIONS

**Rakhesh Singh Kshetrimayum**
Department of Electronics and Communication Engineering, Indian Institute of Technology, Guwahati, Guwahati 781039, India;
Corresponding author: krs@iitg.ernet.in

*Received 23 October 2008*

**ABSTRACT:** *In this article, we have investigated printed double-T monopole antennas for triband applications. A close form formula for calculating the antenna resonance frequency is reported. Such printed monopole antennas are compact, less fragile, planar, and easy for design and fabrication.* © 2009 Wiley Periodicals, Inc. Microwave Opt Technol Lett 51: 1640–1642, 2009; Published online in Wiley InterScience (www.interscience.wiley.com). DOI 10.1002/mop.24446

**Key words:** *printed monopole antenna; multiband antenna; wireless communications*

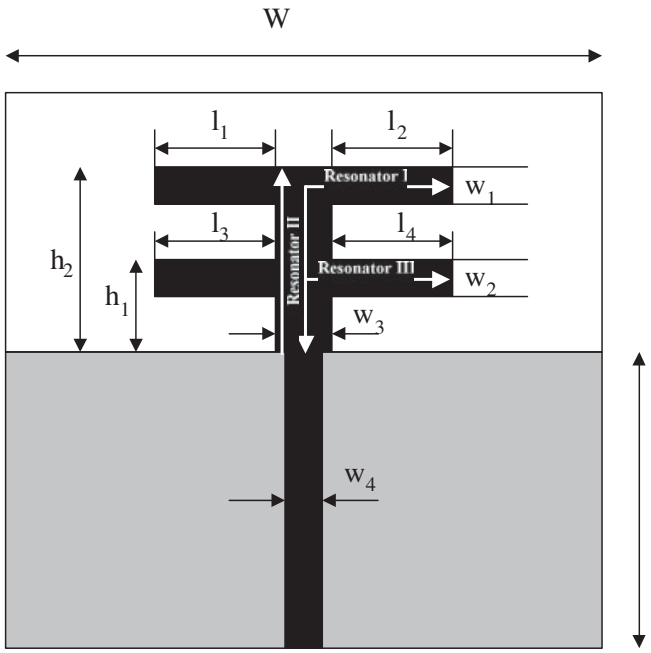


**Figure 1** Geometry of the double-T printed monopole antenna

## 1. INTRODUCTION

An antenna is a transducer designed to transmit or receive electromagnetic waves. It converts electromagnetic waves into electric current and vice versa [1]. Antenna is a very important part of any wireless systems. It is the device from which any signal is radiated into free space. Most antennas usually work in single frequency band. Antennas, which can work properly in more than one frequency regions, are termed as Multiband antennas [2, 3].

Triband antennas as the name suggests could properly function in three frequency bands. The frequency regions, where antennas works as an effective radiator of electromagnetic waves are the frequency regions, where the antenna reflection coefficient, $S_{11}$ is below $-10$ dB. Multiband antennas are generally much more complex than the single band antennas in their design, structures, and operations. In this article, we will investigate printed double-T monopole antenna whose geometry is depicted in Figure 1 which are very simple in design and fabrication but has excellent performance for triband applications.

## 2. PRINTED DOUBLE-T MONOPOLE ANTENNAS: EXPERIMENTAL AND SIMULATION RESULTS

The length of the resonator I is $h_2 - w_1/2 + w_3/2 + l_2$, resonator II is $h_2$, and resonator III is $h_1 - w_2/2 + w_3/2 + l_4$ (refer to Fig. 1). All the resonators were resonating approximately at

$$f = \frac{c\sqrt{(\varepsilon_r + 1)/2}}{8l} \tag{1}$$

where $l$ is the length of each resonator. The dimensions of the printed monopole antenna using FR4 substrate ($\varepsilon_r = 4.4$, thickness = 1.6 mm) were chosen as $W = 75$ mm, $L = 50$ mm, $w_1 = w_4 = 3.2$ mm, $w_2 = w_3 = 3.5$ mm, $h_2 = 14.5$ mm, $h_1 = 5$ mm, $l_1 = l_2 = 5.3$ mm, $l_3 = l_4 = 7.3$ mm. The calculated values for the three resonances are 2.96 GHz, 4.23 GHz, and 5.01 GHz, respectively, which is quite close to the experimentally obtained resonance frequencies (refer to Fig. 2). Note that this formula has been verified for various dimensions and substrate parameters of the printed double-T monopole antenna using IE3D simulation [4] results which has not be reproduced here for the sake of brevity. So this formula can be used for designing printed double-T monopole antenna for triband applications. Author has not come across any close form formula for calculating resonance of such antennas in the literature. Note that $l_1 = l_2$ and $l_3 = l_4$ thereby there is one additional resonance for resonator I and resonator III from the left branch of the antenna, and this enhances the resonance and bandwidth (BW) at the same frequency of operation we have calculated and measured experimentally.

The $S_{11}$ versus frequency for the fabricated printed monopole antenna is obtained using Network Analyzer (see Fig. 2). Note that this printed monopole antenna can work well for triband applications, viz. 2.95 GHz ($S_{11}$: $-24.5$ dB, BW: 0.52 GHz), 4.18GHz ($S_{11}$: $-35.2$ dB, BW: 0.68 GHz), 5.05 GHz ($S_{11}$: $-15.3$ dB, BW: 0.26 GHz). The other antenna parameters were quite similar to other printed monopole antennas reported in [5–8] for various applications such as wireless local area network, ultra wideband, etc will not be discussed in detail. Readers could always refer to the above mentioned papers for similar other antenna parameters.

It has been observed that the E-Plane radiation pattern from the IE3D simulation is like a doughnut or "8" shaped at 2.95 GHz as depicted in Figure 3(a) and similar patterns were observed at 4.18 GHz and 5.05 GHz frequency bands which will not be reproduced here. Because of the unavailability of the antenna pattern measurement facilities as of now, we have used the IE3D simulation software to generate the antenna radiation patterns. We believe that the Method of Moments (MoM) based IE3D software gives radiation pattern of antennas fairly accurate [4].

The antenna radiation patterns at the two higher frequencies were slightly tilted (main beam direction was, respectively, at 0°, 5°, and 10° for radiation pattern at 2.95 GHz, 4.18 GHz, and 5.05 GHz). It is observed that the H-plane radiation patterns are constant for all angles and looks like a circle giving omni directional radiation pattern of the antenna at 2.95 GHz as shown in Figure 3(b) and also at 4.18 GHz, but little distortion is observed at 5.05 GHz.

The cross-polarization at the higher frequency was observed to be higher than at the antenna lower operating frequency (The maximum cross-polarization at 2.95 GHz was less than $-20$ dB whereas at 5.05 GHz, it was less than $-10$ dB). With proper

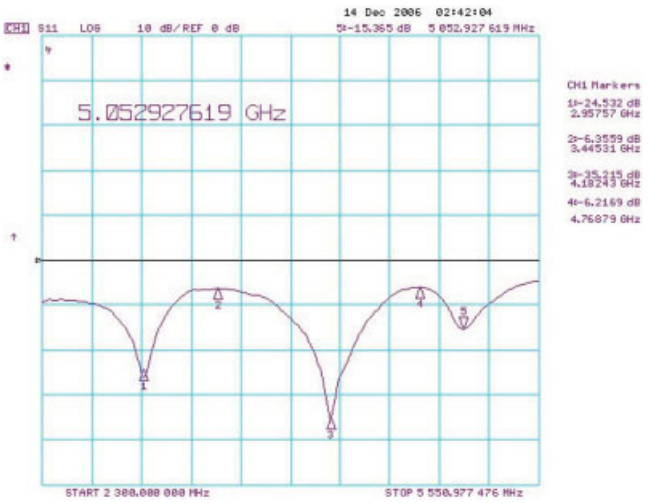


**Figure 2** $S_{11}$ vs. frequency of fabricated printed double-T monopole antenna. [Color figure can be viewed in the online issue, which is available at www.interscience.wiley.com]

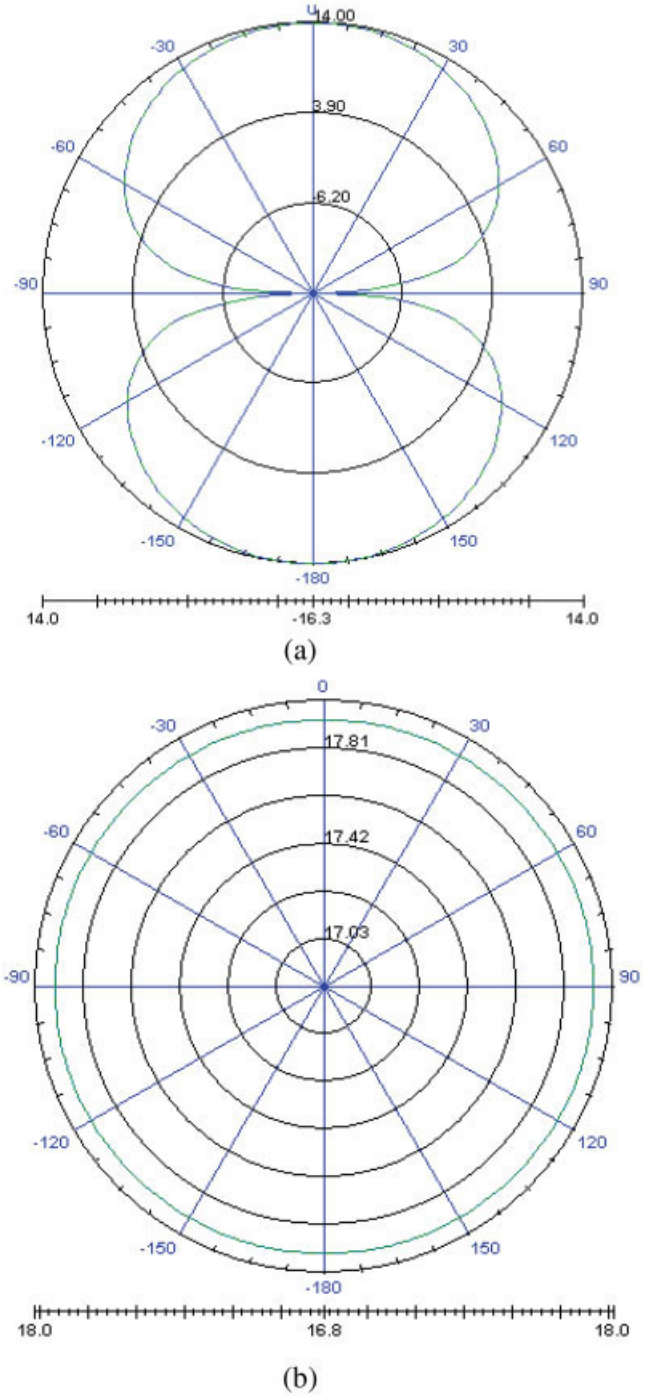


**Figure 3** (a) E-plane and (b) H-plane radiation patterns at 2.95 GHz. [Color figure can be viewed in the online issue, which is available at www.interscience.wiley.com]

impedance matching, the antenna radiating power and radiation intensity were found to be quite good. The efficiency of the antenna was found to be above 80%.

### 3. CONCLUSION

Today's world is the world of wireless communications. All communications are becoming wireless. Antenna is the device which sends out signals into free space for wireless communications. By application of reciprocity theorem, the same antenna could be used either as receiving or transmitting antennas. In general, most of the antennas work in single frequency band. But for multiband antennas, a single can work properly for multiple frequency bands. For that matter, Triband antennas can radiate and receive electromagnetic energy in three frequency bands. In this article, we have investigated printed double-T monopole antennas with the etched ground plane for triband wireless applications. The main contribution of this article is that we have come up with a close form formula for calculating the antenna resonance frequencies in all the three frequency bands which is verified experimentally as well as using IE3D simulation results. Using this close form formula, antenna engineers could design the frequency band of interest directly simplifying their design process to a great extent. Such printed antennas are compact and has simple fabrication process, low-cost, and indeed a very versatile candidate for multiband applications.

### ACKNOWLEDGMENTS

The author acknowledges his students A. Dwivedy and A. Arya for simulation and fabrication of the printed monopole antennas and U. Sarma for helping in obtaining the experimental results.

### REFERENCES

1. C.A. Balanis, Antenna theory: analysis and design, Wiley, New York, NY, 1996.
2. G.R. Dejean, Compact broadband and multiband antenna design for millimetre-wave applications, Vdm Verlag Dr. Mueller E.K., Germany, 2008.
3. G. Kumar and K.P. Ray, Broadband microstrip antenna, Artech House, Norwood, MA, 2003.
4. IE3D version 10.2, Zeland Corp., Freemont, CA.
5. Y.-L. Kuo and K.-L. Wong, Printed double-T monopole antenna for 2.4/5.2 GHz dual-band WLAN operations, IEEE Trans Antennas Propag 51 (2003), 2187–2192.
6. K.P. Ray and Y. Ranga, Printed rectangular monopole antennas, Proc. IEEE Antennas and Propagation Society International Symposium, July 2006, pp 1693–1696.
7. M. John and M.J. Ammann, Optimization of impedance bandwidth for the printed rectangular monopole antenna, Microwave Opt Technol Lett 47 (2005), 153–154.
8. R.S. Kshetrimayum and R. Pillalamarri, Novel UWB printed monopole antenna with triangular tapered feed lines, IEICE Electron Exp 5 (2008), 242–247.



## ELIMINATION OF THE DEPENDENCY OF THE CALIBRATION PLANE AND THE SAMPLE THICKNESS FROM COMPLEX PERMITTIVITY MEASUREMENTS OF THIN MATERIALS

**U. C. Hasar[1,2] and O. E. Inan[3]**
[1] Department of Electrical and Electronics Engineering, Ataturk University, Erzurum 25240, Turkey; Corresponding author: ugurcem@atauni.edu.tr
[2] Department of Electrical and Computer Engineering, Binghamton University, Binghamton, NY 13902
[3] Department of Systems Engineering, Microwave Electronic Systems, Inc. (MIKES), Ankara 06750, Turkey

*Received 23 October 2008*

**ABSTRACT:** *In nonresonant broadband measurements, thin samples do not fill the entire sample holder (a waveguide or coaxial-line section). In this circumstance, the measured scattering parameters have to*